Kinetics of Formation of Di-D-fructose Dianhydrides during Thermal Treatment of Inulin

Ted J. Christian and Merilyn Manley-Harris*

Chemistry Department, University of Waikato, Private Bag 3105, Hamilton, New Zealand

Richard J. Field

Chemistry Department, University of Montana, Missoula, Montana 59812

Beverly A. Parker

Shafizadeh Center, University of Montana, Missoula, Montana 59812

Thermal treatments of solid mixtures of inulin and citric acid result in the formation of di-D-fructose dianhydrides and oligomers derived therefrom. The kinetics of formation of these compounds have been investigated and simulated in computer studies. A mechanism is proposed. The conditions used in this study were analogous to the conditions pertaining to the roasting of chicory, during which similar compounds are formed.

INTRODUCTION

Thermal treatments of anhydrous, acidified inulin yielded a caramel containing 13 di-D-fructose dianhydrides (DFDAs), of which 12 were unequivocally identified (Manley-Harris and Richards, 1996). The caramel also yielded oligomers shown by electrospray mass spectroscopy to consist of di-D-fructose dianhydrides to which glycosyl units are appended. Trimers of this type were isolated and characterized from caramels formed in analogous treatments of sucrose.

Chicory, derived from the root of *Cichorium intybus* L. var. *sativum* DC., is dried and roasted for use as a coffee additive, predominantly in Europe, or as a coffee substitute in a variety of health food beverages. The main storage polysaccharide of chicory is inulin, and up to 3% of organic acids have also been identified in chicory roots (Pazola, 1985). Four di-D-fructose dianhydrides have been isolated as the per-*O*-acetates from a preparation of roasted chicory (Defaye and Fernández, 1995). These authors also indicated the possible presence of higher oligomers of fructose and di-D-fructose dianhydrides in the roasted chicory.

Caramels containing di-D-fructose dianhydrides and oligomers thereof have been found to have prebiotic qualities during animal trials (Orban et al., 1997). A prebiotic is an oligosaccharide, which, being indigestible by humans or other animals, passes into the colon, where it is fermented by certain beneficial species in the colonic microflora. This brings about a selective enhancement of beneficial bacteria with commensurate health benefits to the host (Gibson and Roberfroid, 1995).

In this study anhydrous, acidified inulin has been thermolyzed under carefully controlled conditions to study the kinetics of formation of di-D-fructose dianhydrides. A further two di-D-fructose dianhydrides have been identified, one of which forms transiently, bringing the total to 14. The kinetics have been modeled using computer simulations, and a mechanism is proposed. Examination of commercial chicory samples showed that roasts of differing duration conformed to the results observed in this study.

EXPERIMENTAL PROCEDURES

Materials and General Procedures. Inulin (from dahlia tubers, Sigma) and citric acid (Aldrich) were purchased and used without further purification. The certificate of analysis for the inulin indicated <0.05% each of free fructose and free glucose and a fructose/glucose ratio of 31:1.

Gas Chromatography (GC-FID) and Gas Chromatography–Mass Spectrometry (GC-MS). GC-FID was effected using a Hewlett-Packard 5890 series A gas chromatograph with an on-column injector fitted with a cross-linked 5% phenyl-dimethyl siloxane column (HP Ultra-2, 25 m × 0.33 mm × 0.53 μm). GC-MS was effected using either the above column or a 100% dimethyl siloxane (HP-1, 25 m × 0.33 mm × 0.53 μm) column installed in a Hewlett-Packard 5890 series A gas chromatograph with direct interface to an HP 5970 mass spectral detector (70 eV). The temperature program for both GC methods was 55 °C for 1 min, 30°C/min to 170 °C, 3 °C/min to 320 °C, and hold for 10 min. Total acquisition time was 65 min.

Liquid Chromatography (LC). Four LC methods were employed.

Method i. Preparative LC was performed on aqueous samples (~1 g/mL) using Waters Delta Pak C$_{18}$ cartridges (3–25 × 100 mm, 15 μm, 100 Å, plus guard pak) eluted at 10.0 mL/min with H$_2$O.

Method ii. Analytical LC was performed using (a) a Waters Resolve C$_{18}$ Radial Pak cartridge (8 × 100 mm, 5 μm, plus guard pak) eluted at 1.0 mL/min with H$_2$O or (b) a Phenomenex Resex RCM-Monosaccharide (8% cross-linked, Ca^{2+}) column eluted with water at 80 °C and 0.6 mL/min. Waters 515 HPLC pumps and a Waters 410 differential refractometer were used with these two systems.

* Author to whom correspondence should be addressed (e-mail manleyha@waikato.ac.nz; fax +64-7-838-4219).

1824 *J. Agric. Food Chem.,* Vol. 48, No. 5, 2000

Christian et al.

Method iii. A Dionex high-performance anion exchange HPLC system with pulsed electrochemical detection (HPAE-PED) was used to examine the inulin profile. Elution was by sodium hydroxide/sodium acetate gradient (NaOH/NaAc) at 1.0 mL/min. Eluents were made up by dissolving weighed amounts of reagent grade NaAc·3H$_2$O in degassed, ultrapure water (>17 MΩ cm^{-1}) and adding measured volumes of reagent grade certified 50% NaOH solution. The column was a Dionex CarboPac PA1. The gradient profile was from 95% A/5% B at 0 min to 100% B at 60 min, where A was 150 mM NaOH and B was 150 mM NaOH/500 mM NaAc. Detector electrode potentials were +0.10 V (0−0.5 s), +0.60 V (0.51−0.60 s), −0.60 V (0.61−0.65 s) with an integration period of 0.30−0.50 s. The method included 10 min equilibration times at the beginning and end of each run. The reference electrode was Ag/AgCl, and acquisition was via analog/digital interface to Dionex AI-450 chromatography software.

Method iv. Size exclusion chromatography (SEC) was performed on a Pharmacia glass column (2.6 × 90 cm ≈ 475 mL) packed with Bio-Rad Bio-Gel P-2 ultrafine (<45 μm) medium eluted with H$_2$O at 0.5 mL/min. The refractive index detector (Waters 410) output was amplified and routed through a PICO AD-100 analog to digital converter to a DOS-based computer. Acquisition time was ~15 h.

Electrospray Mass Spectrometry (ES-MS). ES-MS was carried out using a Fisons Instrument VG Platform II mass spectrometer with MeOH as the mobile phase eluted at 0.02 mL/min. The spectrometer probe temperature was 60 °C and the cone voltage +180 V. Samples were spiked with NaCl to assist ionization.

Nuclear Magnetic Resonance (NMR) Spectrometry. NMR spectra were obtained using a Brüker ADV DRX400 400 MHz spectrometer in D$_2$O (CDCl$_3$ for per-*O*-acetates) referenced to internal *t*-BuOH at 1.2 and 31.6 ppm (or in CDCl$_3$ referenced to CDCl$_3$ at 7.26 and 77.0 ppm). ^{1}H, ^{13}C, DEPT, H,H−COSY, HSQC, and HMBC experiments were carried out. For HSQC a *J* value of 145 Hz was used, and for HMBC a delay value of 80 ms was used for evolution of long-range couplings.

Methylation Analyses. Samples were methylated with NaOH and MeI in Me$_2$SO after the method of Ciucanu and Kerek (1984) with modifications to the procedure as described by Needs and Selvendran (1993). Methylated samples were hydrolyzed by a moderate hydrolysis procedure (Manley-Harris and Richards, 1993) and reduced (NaBD$_4$) and acetylated after the method of Blakeney et al. (1983).

Preparation of 1-Kestose and Nystose. 1-Kestose [β-D-fru*f*-(2→1)-β-D-fru*f*-(2↔1)-α-D-GLC*p*] and nystose [β-D-fru*f*-(2→1)-β-D-fru*f*-(2→1)-β-D-fru*f*-(2↔1)-α-D-GLC*p*] were isolated from the commercial product Nutraflora (Golden Technologies, Inc., Golden, CO) using LC method i. 1-Kestose and nystose are the only major components of this product detectable by standard GC-FID and reversed phase LC methods and are easily resolved. Their identities were confirmed by comparison of ^{13}C spectra with published values (Bock et al., 1984). They are hygroscopic and required storage under vacuum over phosphorus pentoxide (P$_2$O$_5$) at 40 °C for 48 h or more to remove water after freeze-drying. Continued storage under vacuum over a desiccant was sufficient to keep the samples dry.

α-D-Fructopyranose-β-D-fructopyranose 1,2′:2,1′-dianhydride, α-D-fructofuranose-β-D-fructopyranose 1,2′:2,1′-dianhydride, β-D-fructofuranose-β-D-fructopyranose 1,2′:2,1′-dianhydride, and di-β-D-fructopyranose 1,2′:2,1′-dianhydride were prepared after the method described by Hilton (1963) but with chromatographic separation by LC method i. Their identities were confirmed by comparison of the NMR spectra with the literature (Angyal and Bethell, 1976; Defaye and Fernández, 1992).

α-D-Fructofuranose-β-D-fructofuranose 1,2′:2,1′-dianhydride was prepared from a large-scale thermolysis of inulin and 1.5% citric acid by successive preparative LC using LC method i. The identity of α-D-fructofuranose-β-D-fructofuranose 1,2′:2,1′-dianhydride was confirmed by comparison with the NMR spectrum with the literature (Defaye and Fernández, 1992).

α-D-Fructofuranose-β-D-fructofuranose 1,2′:2,6′-dianhydride was isolated from early-stage thermolysis mixtures by re-

peated preparative LC using LC methods i and iib. Methylation analysis yielded only 1,2,5-tri-*O*-acetyl-3,4,6-tri-*O*-methyl-2-(^{2}H)mannitol and glucitol and 2,5,6-tri-*O*-acetyl-1,3,4,-tri-*O*-methyl-2-(^{2}H)mannitol and glucitol, which are co-incident by GC but distinguishable by MS (Carpita and Shea, 1988). ^{13}C NMR shifts (D$_2$O; ppm): 108.2 (C-2), 105.1 (C-2′), 82.8 (C-3), 78.2 (C-4), 83.2 (C-5), 80.1 (C-3′), 75.8 (C-4′), 83.6 (C-5′), 62.6 (C-1), 61.1 (C-1′), 58.4 (C-6), 62.1 (C-6′). ^{1}H NMR shifts (D$_2$O; ppm): 3.964 (H-1a, $J_{1a,1b}$ = 14.4 Hz), 3.68 (H-1b), 3.515 (H-1′a, H-1′b, $J_{1′a,1′b}$ ~ 0 Hz), 4.033 (H-3, $J_{3,4}$ = 3.2 Hz), 3.840 (H-4, $J_{4,5}$ = 6.3 Hz), 3.895 (H-5, $J_{5,6}$ = 3.2 Hz), 4.101 (H-3′, $J_{3′,4′}$ = 6.4 Hz), 4.574 (H-4′, $J_{4′,5′}$ = 4.4 Hz), 4.021 (H-5′, $J_{5′,6′a}$ = 2.8), 3.761 (H-6a, H-6b, $J_{6a,6b}$ ~ 0 Hz), 3.76 (H-6′a, H-6′b, $J_{5′,6′b}$ = 5.6 Hz, $J_{6′a,6′b}$ = 12.4 Hz).

α-D-Fructofuranose-β-D-fructofuranose 1,2′:2,6′-dianhydride was per-*O*-acetylated to yield a crystalline acetate, mp = 113 °C [lit. value = 113 °C (Matsuyama et al., 1991)]. ^{13}C NMR shifts (CDCl$_3$; ppm) of per-*O*-acetate: 107.0 (C-2), 102.7 (C-2′), 80.2 (C-3), 77.6 (C-4), 79.4 (C-5), 78.2 (C-3′), 78.0 (C-4′), 82.9 (C-5′), 57.7 (C-1), 63.2 (C-1′), 63.1 (C-6), 61.8 (C-6′). ^{1}H NMR shifts (CDCl$_3$; ppm) of per-*O*-acetate: 3.893 (H-1a, $J_{1a,1b}$ = 13.4 Hz), 3.691 (H-1b), 4.017 (H1′a, $J_{1′a,1′b}$ = 11.9 Hz), 4.063 (H-1′b), 5.334 (H-3, $J_{3,4}$ = 2.4 Hz), 4.894 (H-4, $J_{4,5}$ = 5.7 Hz), 4.108 (H-5, $J_{5,6a}$ = 2.8 Hz), 5.371 (H-3′, $J_{3′,4′}$ = 5.1 Hz), 5.484 (H-4′, $J_{4′,5′}$ = 3.2 Hz), 4.069 (H-5′, $J_{5′,6′a}$ = 0.8 Hz), 4.365 (H-6a, $J_{5,6b}$ = 5.6 Hz), 4.132 (H-6b, $J_{6a,6b}$ ~ 15 Hz), 3.963 (H-6′a, $J_{5′,6′b}$ = 2.3 Hz), 3.853 (H-6′b, $J_{6′a,6′b}$ = 14.1 Hz).

Commercial Chicory. Samples of roasted chicory and instant chicory powders were kindly supplied by Leroux S.A. (Orchies, France). The roasted chicory samples were extracted with MeOH overnight at 25 °C and filtered, and the filtrate was taken to dryness under vacuum. The extracts were redissolved in water for SEC. Instant chicory powders were dissolved directly in water for SEC. All samples were fractionated by SEC and the fractions examined by ES-MS. Instant chicory powders were dissolved in pyridine and silylated for GC-FID.

Thermolyses of Inulin, Nystose, and Individual Di-D-fructose Dianhydrides.

Preparation of Starting Material. To obtain 1.5% citric acid by weight, inulin and milled citric acid were dissolved independently in ratios of 19.70 g of inulin in ~300 mL of water and 0.30 g of citric acid in ~10 mL of water. The inulin solution was heated to ~50 °C and allowed to cool to room temperature. Once cool, the two solutions were combined, mixed thoroughly by stirring, and freeze-dried immediately to yield an inulin/citric acid powder. The process was repeated with appropriate amounts to obtain citric acid concentrations of 1.0, 2.0, and 2.9 wt %. Similar procedures were employed to prepare mixtures of citric acid with nystose and with individual di-D-fructose dianhydrides.

Thermolysis. Thermolyses were performed in Teflon-lined, screw-capped glass vials immersed in silicone oil (polymethylphenylsiloxane) at 160−180 °C. Temperature was maintained to within ±0.2 °C with a thermostated recirculating pump. A bank of nine screw-cap vials, each containing ~10 mg (accurately weighed to ±0.01 mg) of inulin/citric acid powder, was lowered into the heated silicon oil. At timed intervals, each vial was withdrawn and plunged immediately into ice water.

Derivatization. Immediately after a thermolysis experiment had been completed, all nine samples were dissolved with sonication in 0.75 mL of pyridine. To each was then added 100 μL of internal standard (~6 ± 0.01 mg/mL xylitol in pyridine) and 0.25 mL of neat chlorotrimethylsilane. The samples were quickly capped, held at 100 °C for 1 h, and then allowed to cool to room temperature. Pyridine was blown off with dry nitrogen at room temperature and replaced with 2 mL of *n*-hexane that had been glass distilled. The samples were sonicated for 10 min, centrifuged for 5 min at 1.5 × 10^3*g*, and filtered. The final samples were stored below 0 °C in clean vials while awaiting GC analysis.

Analysis. Samples were analyzed by GC-FID. Response factors (RF) for four individual di-D-fructose dianhydrides (α-D-fructopyranose-β-D-fructopyranose 1,2′:2,1′-dianhydride, α-D-fructofuranose-β-D-fructopyranose 1,2′:2,1′-dianhydride, α-D-fructofuranose-β-D-fructofuranose 1,2′:2,1′-dianhydride, and

Kinetics of Difructose Dianhydride Formation in Thermolysis of Inulin

J. Agric. Food Chem., Vol. 48, No. 5, 2000 **1825**

β-D-fructofuranose-β-D-fructopyranose 1,2′:2,1′-dianhydride), at concentrations similar to those encountered in the experiments, were determined relative to the internal standard xylitol. The average RF (0.60) was applied to all di-D-fructose dianhydrides.

Data Analysis and Kinetic Modeling. *Quantitation.* GC-FID integration results were obtained with an HP Chem-Station for each sample. These were then imported into a graphics package (Axum, MathSoft, Inc., version 5.0) for calculation of percent conversion and for graphical treatment.

Preliminary Curve-Fitting. Initial estimates for the rate of formation and disappearance of each DFDA were obtained in Axum using a nonlinear least-squares routine. The algorithm combines Taylor Series or the Gauss−Newton method with the gradient, or steepest descent, method (Cuthbert et al., 1971). The rate equation used in this part of the study was

$$[I]_n = \frac{k_n[\text{inulin}]_0}{k'_n - k}(e^{-kt} - e^{-k_n t}) \qquad (1)$$

where $[I]_n$ is the concentration at any time of the individual DFDA that is under scrutiny, $[\text{inulin}]_0$ is the initial inulin concentration, and k, k_n, and k'_n are the rate constants for the disappearance of inulin, individual DFDA formation, and individual DFDA decay, respectively. The origin of this equation is discussed below. Nonlinear curve-fitting was used in this study as a rough estimate only of rate constants.

Kinetic Modeling. Computer models of tentative kinetic mechanisms were developed using SIMSODE (L. Gyorgi, Eotvos Lorand University, Budapest, Hungary, personal communication, 1990), a numerical simulation program for chemical reaction systems with mass-action kinetics. The program invokes LSODE, the Livermore Solver for Ordinary Differential Equations (A. C. Hindmarsh, Lawrence Livermore National Laboratory, Livermore, CA, 1981), to calculate a solution based on user-specified mechanisms and rate constants. SIMSODE writes an ASCII file containing concentration/time data for each species in the mechanism. These data were then imported into Axum and visualized graphically.

RESULTS AND DISCUSSION

The di-D-fructose dianhydrides (DFDAs) have been the subject of a recent review (Manley-Harris and Richards, 1997). The abbreviated nomenclature suggested in that review will be used in this discussion. Figure 1 shows the 14 di-D-fructose dianhydrides that have been identified in the products of the thermolysis of inulin together with the appropriate abbreviated names. An indication of previous nomenclature is also given, where DFA and DHL stand for the historically used names difructose anhydride and diheterolevulosan, respectively.

Of the 14 di-D-fructose dianhydrides shown in Figure 1, 12 had been previously identified in inulin thermolyses (Manley-Harris and Richards, 1996); α-D-Fruf-1,2′:2,6′-β-D-Fruf, **3** (Mazama et al., 1991), and β-D-Frup-1,2′:2,1′-β-D-Frup, **14** (Angyal et al., 1990), although previously known in other contexts, have now been identified for the first time as products of the thermolysis of inulin. **14** has also been identified recently in a fructose caramel (Ratsimba et al., 1999). The NMR spectra of both **3** and **14** concurred with the literature, although some of the signals in the spectra of **3** have been reassigned. An interesting feature of the ^{1}H spectrum of **3** was the equivalence of the pairs of diastereotopic protons attached to C-6 and C-1′. This equivalence disappears upon acetylation. Usually in di-D-fructose dianhydrides, in which the central

dioxane ring is conformationally constrained, these protons each show widely separated shifts and display geminal coupling unlike some singly linked disaccharides such as sucrose. Presumably the larger central trioxacane ring leads to a more flexible structure and a situation approaching a singly linked disaccharide; this flexibility must be lost upon acetylation.

Total DFDAs from Thermolysis of Inulin plus 1.5% Citric Acid at 160°C. The data for inulin/1.5% citric acid thermolysis at 160 °C are presented in Figure 2. Conversion of inulin to total DFDAs reaches a maximum of ∼35 wt % after 25 min. (Conversion is expressed as the percentage weight of DFDAs relative to the starting weight of inulin. Total conversion is the sum of weight percent conversion values for all DFDAs in a sample.) This rapid conversion is followed by a much slower degradation, which appears to end after ∼30 h. Degradation may be to nonspecific products, but loss may also occur by glycosylation of DFDAs to yield trimers and higher oligomers. Such species have been demonstrated previously in thermolyses (Manley-Harris and Richards, 1996; Defaye and Fernández, 1995) and are documented in this study by SEC and ES-MS.

Individual DFDAs from Inulin plus 1.5% Citric Acid at 160°C. The relative distribution of DFDAs throughout the thermolysis of inulin/1.5% citric acid at 160 °C is shown in Figure 3. DFDAs are sorted in this figure, for convenience only, from front to back in order of least abundant to most abundant at 30 min into the reaction. The right-hand axis, labeled "DFDA", reflects this sorting. Note that α-D-Frup-1,2′:2,1′-β-D-Frup, **6**, and β-D-Fruf-1,2′:2,1′-α-D-Frup, **7**, are listed together because they were not resolved on the GC-FID.

The relative abundance of any individual DFDA is a balance between its rate of formation and its rate of disappearance. A possible mechanism for the formation of DFDAs from inulin, a modification of that proposed by Blize et al. (1994), is shown in Scheme 1. This mechanism predicts that the most readily formed products will contain at least one β-furanose moiety, and indeed at 2 min α-D-Fruf-1,2′:2,3′-β-D-Fruf, **1**, α-D-Fruf-1,2′:2,6′-β-D-Fruf, **3**, β-D-Fruf-1,2′:2,3′-β-D-Fruf, **5**, α-D-Fruf-1,2′:2,1′-β-D-Fruf, **10**, and β-D-Fruf-1,2′:2,1′-β-D-Fruf, **12**, are the most abundant DFDAs. The fact that the three most abundant species after 2 min (**1**, **3**, and **10**) all contain an α-linkage may indicate a degree of steric hindrance by the C-3 OH, with subsequent greater propensity for the incoming hydroxyl group to attack on the lower face of the sp² hybridized anomeric carbon. Cleavage of the dimer from the inulin oligomer may occur before or after DFDA formation.

The absence of pyranose in these early products is not surprising. In addition to being attacked immediately by neighboring hydroxyl groups, a terminal fructofuranosyl cation can adopt a 2,6-anhydro-β-D-fructofuranose form. This anhydro form is in equilibrium, not only with the furanosyl cation but with a pyranosyl cation, which is less stable than the furanosyl for conformational reasons. Thus, formation of the pyranose-containing DFDAs requires an additional step and proceeds through a less stable intermediate.

The mechanism accounts for all of the DFDAs that contain one or more β-D-fructofuranose rings. It is important to note, however, that five DFDAs (α-D-Frup-1,2′:2,1′-β-D-Frup, **6**, α-D-Fruf-1,2′:2,1′-α-D-Fruf, **8**, α-D-Fruf-1,2′:2,1′-β-D-Frup, **9**, α-D-Fruf-1,2′:2,1′-α-D-Frup, **11**, and β-D-Frup-1,2′:2,1′-β-D-Frup, **14**) are still unac-
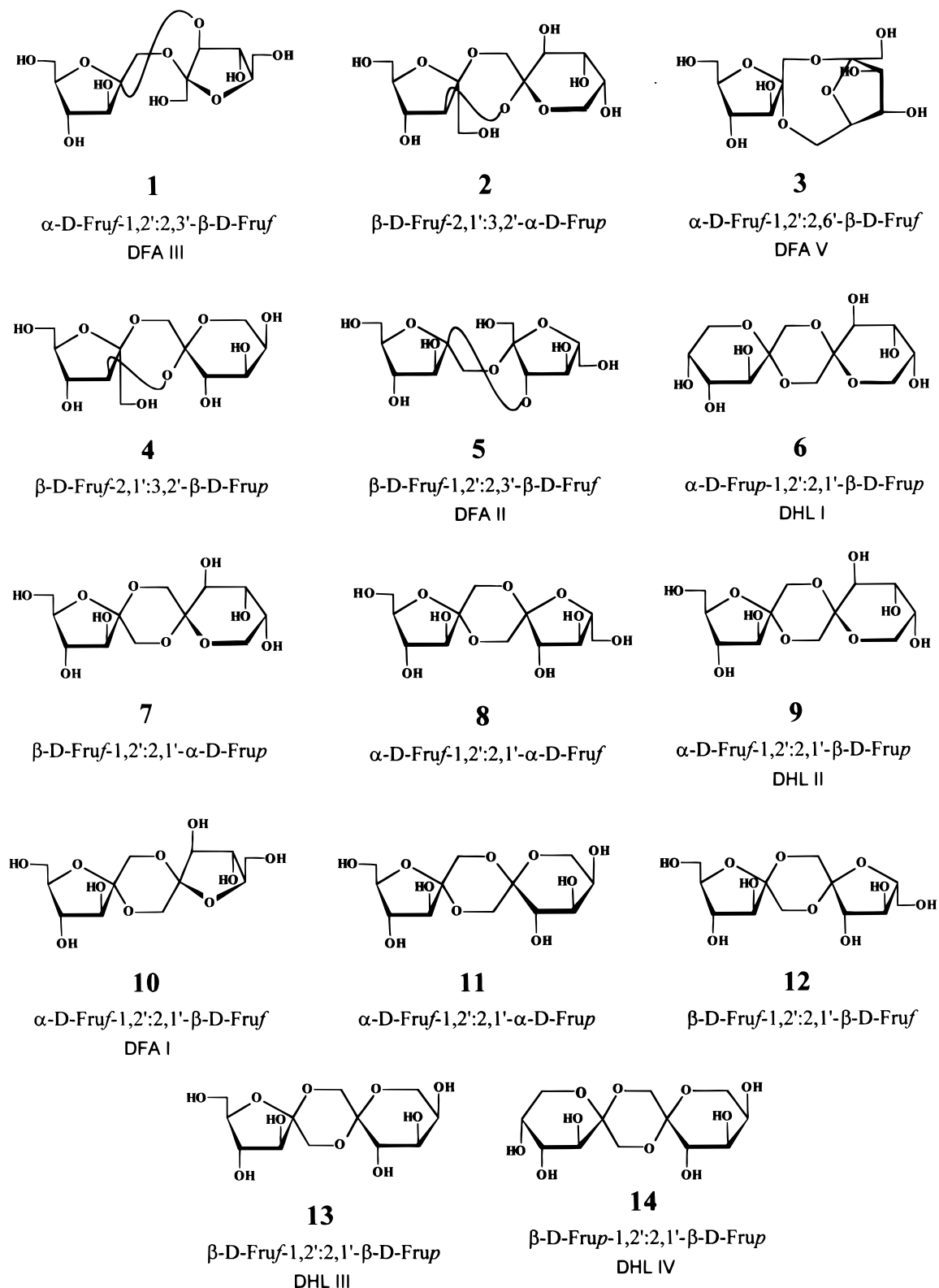
1826 *J. Agric. Food Chem.,* Vol. 48, No. 5, 2000

Christian et al.

1

α-D-Fru*f*-1,2':2,3'-β-D-Fru*f*
DFA III

2

β-D-Fru*f*-2,1':3,2'-α-D-Fru*p*

3

α-D-Fru*f*-1,2':2,6'-β-D-Fru*f*
DFA V

4

β-D-Fru*f*-2,1':3,2'-β-D-Fru*p*

5

β-D-Fru*f*-1,2':2,3'-β-D-Fru*f*
DFA II

6

α-D-Fru*p*-1,2':2,1'-β-D-Fru*p*
DHL I

7

β-D-Fru*f*-1,2':2,1'-α-D-Fru*p*

8

α-D-Fru*f*-1,2':2,1'-α-D-Fru*f*

9

α-D-Fru*f*-1,2':2,1'-β-D-Fru*p*
DHL II

10

α-D-Fru*f*-1,2':2,1'-β-D-Fru*f*
DFA I

11

α-D-Fru*f*-1,2':2,1'-α-D-Fru*p*

12

β-D-Fru*f*-1,2':2,1'-β-D-Fru*f*

13

β-D-Fru*f*-1,2':2,1'-β-D-Fru*p*
DHL III

14

β-D-Fru*p*-1,2':2,1'-β-D-Fru*p*
DHL IV

Figure 1. DFDA structures and shorthand and trivial names.

counted for and must arise from starting material other than inulin oligomers. A possible source for these is free fructose moieties liberated by simple hydrolysis. Free fructose may, of course, also be a source of other DFDAs. Monomeric fructose present in the original inulin would be in the pyranose form. Fructose liberated by hydrolysis would, at least initially, be in the furanose form. The effect of these alternative possible pathways upon modelling is discussed later.

The rapid rate of disappearance of α-D-Fru*f*-1,2':2,6'-β-D-Fru*f*, **3**, is presumably due to the eight-membered central trioxacane ring, which is less stable than the six-membered dioxane ring present in all of the other species.

The relative stability of the pyranose-containing DFDAs compared with those containing only furanose residues may have a twofold cause. First, removal by glycosylation giving rise to higher oligomers is slowed
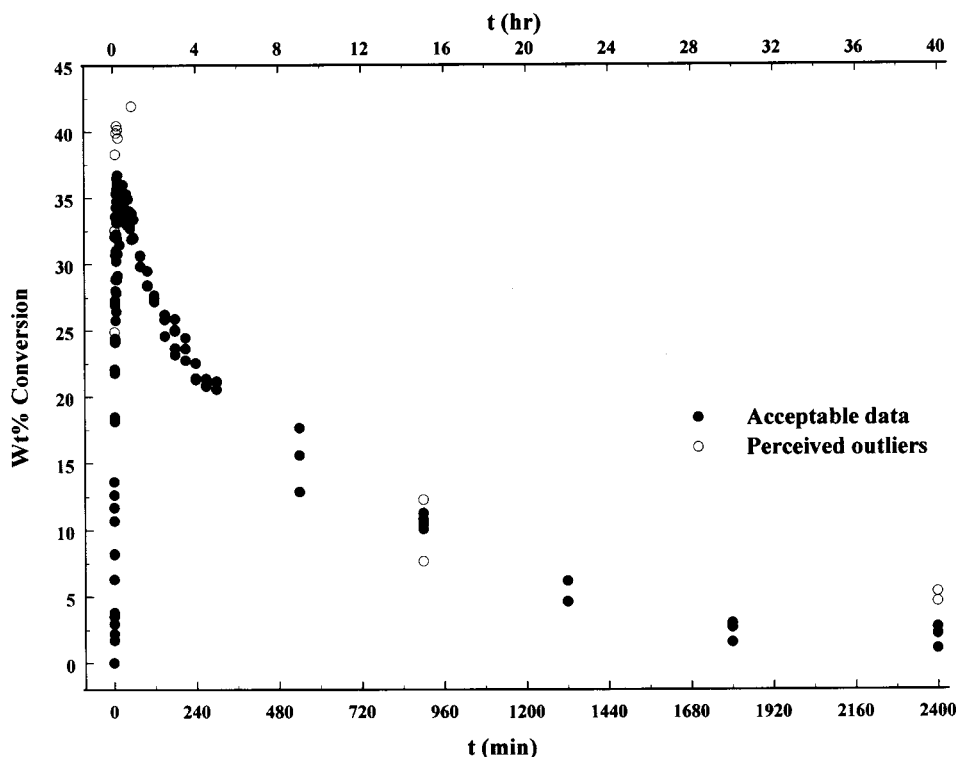
Kinetics of Difructose Dianhydride Formation in Thermolysis of Inulin

J. Agric. Food Chem., Vol. 48, No. 5, 2000 **1827**

Figure 2. Conversion (0–40 h) of inulin/1.5% citric acid to DFDAs at 160 °C.
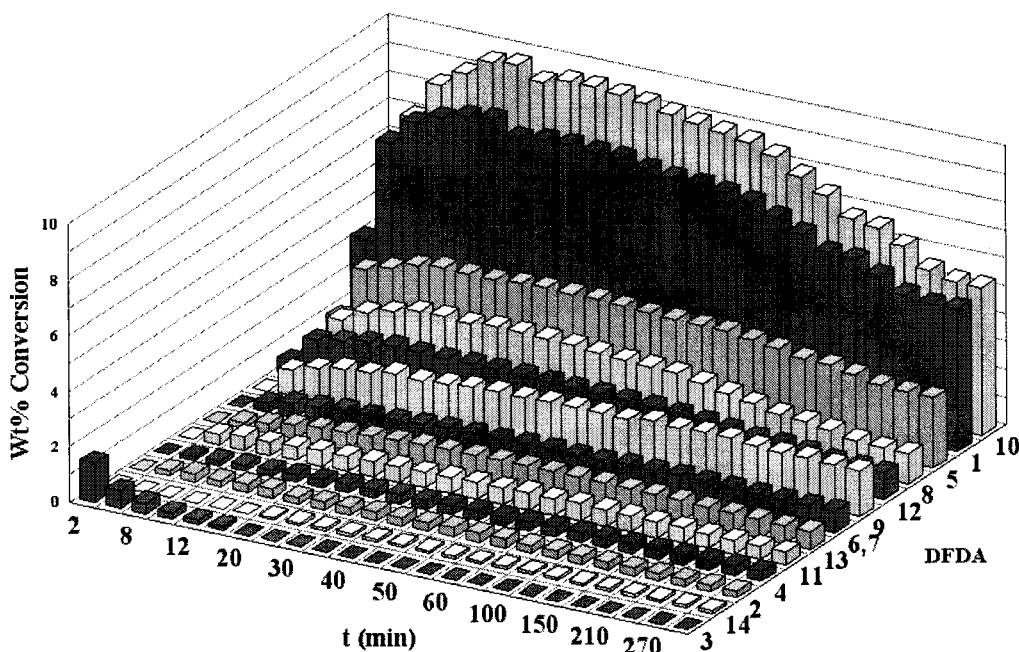

Figure 3. Weight percent individual DFDAs from thermolysis of inulin/1.5% citric acid at 160 °C.

or prevented. The pyranose residue does not have any free primary hydroxyls; for steric reasons it would be expected that attack by a glycosyl cation would occur predominantly at a primary hydroxyl (Manley-Harris and Richards, 1996). Second, if acid hydrolysis occurs by protonation and opening of the dioxane ring to yield a cation, then a pyranose residue would be expected to confer some stability because the formation of a pyranosyl cation would require more energy.

Disappearance of Inulin during Thermolysis. A quantitative determination of the rate of disappearance of inulin was not feasible because inulin consists of a range of oligomers and polymers. However, a qualitative understanding can be gained from HPLC analysis of thermolysis samples using LC method iii. Inulin oligomers and polymers differ only in the number of fructose residues and elute on the Dionex LC system in order of increasing degree of polymerization (dp) (Slaughter and Livingston, 1994; Dionex Corp.). In the untreated inulin sample a range of dps were observed including a large peak at ~3 min, which had the same retention time as D-fructose. Because <0.05% of free fructose is indicated in the certificate of analysis, a possible source for this fructose is hydrolysis occurring during storage or chro-

Scheme 1.   Mechanism for the Formation of DFDAs Directly from Inulin
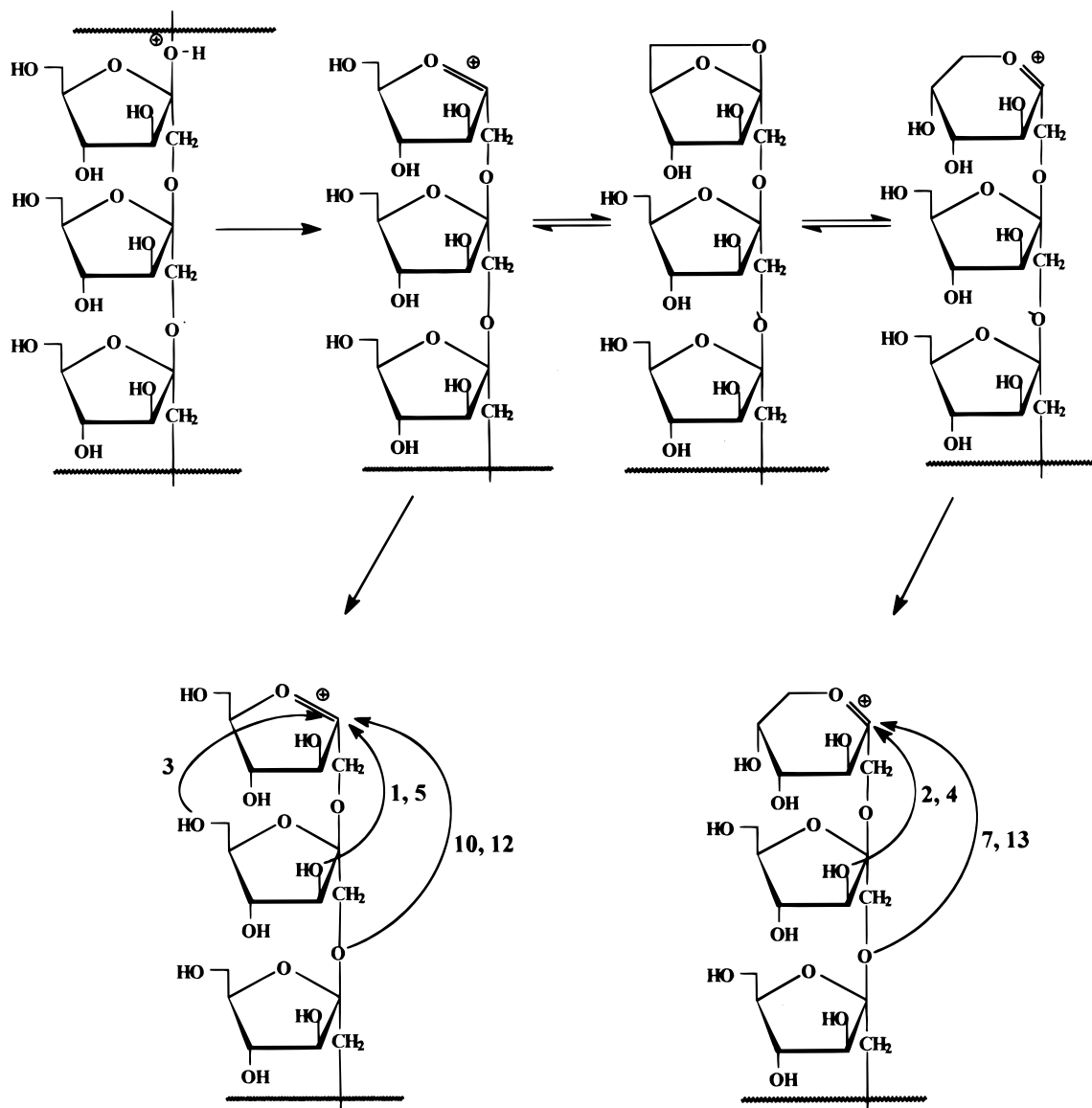
matography. The latter hydrolysis would have to be effected by the chromatographic conditions because free fructose was also observed in inulin without added citric acid. SEC of the inulin using LC method iv revealed that all material was excluded by Bio-Gel P-2 and no monomeric material was observed. The SEC system with detection by refractive index may be less sensitive, however, than the pulsed electrochemical detection.

Figure 4 expands the region of the chromatogram from 0 to 10 min and compares it with standards of DFDAs and mono-, di-, tri-, and tetrasaccharides.

The order of elution of the DFDAs relates to the number of primary hydroxyl groups present; **10**, which has two primary hydroxyl groups, has the longest retention time. From this it is reasonable to infer that peaks that eluted between 10 and 20 min in the thermolysis samples were variously glycosylated DFDAs rather than more labile inulin oligomers. The extreme lability of low-dp inulin oligomers was demonstrated by thermolysis experiments on nystose. At 160 °C and 1.5 wt % citric acid, nystose had completely disappeared within 2 min and a range of DFDAs had formed. A 10-fold decrease in citric acid concentration to 0.17 wt % did not change this result. Only when the reaction

temperature was lowered to 130 °C did nystose react slowly enough for the rate of disappearance to be measured. Thus, the conditions during inulin thermolysis in this study were sufficient to cause complete and rapid removal of low-dp inulin oligomers.

Assuming an initial maximum dp of ∼32 (31 fructose residues terminating in a single glucose residue), it is apparent that inulin fragmentation is extensive and occurs rapidly. The rapid disappearance of inulin—nearly complete, on a qualitative basis, after 15 min—does not coincide with the maximum concentration of DFDAs, which occurs after ∼25 min. The discrepancy between the apparent disappearance of oligomeric starting material and the time after which DFDA decay occurs more rapidly than formation suggests a route to DFDA formation that does not include inulin oligomers.

Three peaks in each of the thermolysis samples corresponded, by retention time, to glucose, fructose, and sucrose. Although retention time alone does not prove these assignments, they were supported by GC-FID analysis. Glucopyranose, fructopyranose, and fructofuranose are present early in relatively large abundance and disappear gradually. Sucrose forms to a lesser extent and is essentially gone after 15 min.
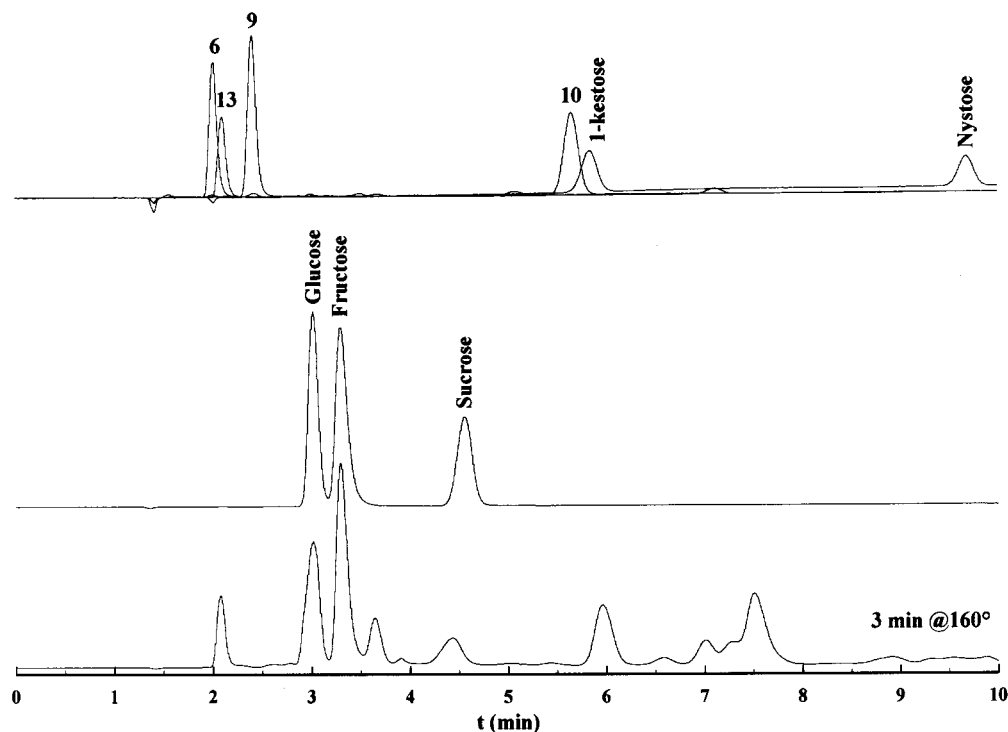
Kinetics of Difructose Dianhydride Formation in Thermolysis of Inulin

J. Agric. Food Chem., Vol. 48, No. 5, 2000 **1829**

Figure 4. Comparison of HPAE-PED chromatograms of a 3 min thermolysis sample with glucose, fructose, sucrose, 1-kestose, nystose, and DFDA standards.

The presence of D-fructose and small amounts of sucrose makes them candidates for source material for the five DFDAs for which the previously proposed mechanism does not account. These five do not contain β-linked fructofuranose and cannot form directly from inulin. Instead, they can arise from the attack of fructopyranose or fructofuranose OH groups on a monomeric fructosyl cation. This cation may also contribute to the formation of the other nine DFDAs, in addition to their formation directly from inulin oligomers, and thus would account for continued formation after all inulin oligomers had disappeared.

Thermolysis of Individual DFDAs. Degradation studies were carried out separately on α-D-Fru*p*-1,2′:2,1′-β-D-Fru*p*, **6**, α-D-Fru*f*-1,2′:2,1′-β-D-Fru*p*, **9**, and α-D-Fru*f*-1,2′:2,1′-β-D-Fru*f*, **10**. This group includes a dipyranose, a furanose–pyranose, and a difuranose dianhydride. Because these samples were isolated by LC, there was a degree of cross-contamination, especially between **6** and **9**, and contamination with other DFDAs and trimers. **6**, **9**, and **10** were each thermolyzed individually in the presence of 1.5 wt % citric acid at 160 °C and the products analyzed by GC-FID of the per-*O*-trimethylsilyl derivatives.

The relative concentration of the dipyranose dianhydride α-D-Fru*p*-1,2′:2,1′-β-D-Fru*p*, **6**, remained > ~95% over a reaction period of 5 h. Thermolysis of the furanose–pyranose dianhydride α-D-Fru*f*-1,2′:2,1′-β-D-Fru*p*, **9**, gave similar results; **9** did not decay after 5 h at 160 °C.

The behavior of α-D-Fru*f*-1,2′:2,1′-β-D-Fru*f*, **10**, was decidedly different from that of **6** and **9** (Figure 5); **10** degraded steadily over the 5 h reaction time. At least five other DFDAs were present in the starting material, but after 30 min, at least 12 of the 14 DFDAs were still present or had formed. The reaction time was extended to 40 h. Note in the insert the increased relative abundance of DFDAs other than **10**. As **10** degrades,

the combined concentration of other DFDAs (▲) in the reaction mixture increases out to 4 h, after which all DFDAs gradually decay to very low abundance.

Once the concentration of **10** falls to a certain level (~5 h), the concentrations of all DFDAs decline steadily. It is possible that **10** isomerizes to other DFDAs or that it decays to products which react further to form other DFDAs, or both. The trimers increase slightly in abundance for the first 30 min and then decrease slowly, although not to the same extent as the other DFDAs; these trimers may originate from, for example, tetramers that coeluted during LC but are not observable in GC. The monomer component arises from degradation to yield fructose. Some nonspecific degradation products, for example, H_2O, CO, CO_2, CH_2O, HMF, and furfural (Goretti et al., 1980; Scheer, 1983; Ponder and Richards, 1993), presumably elute with the solvent in GC or are lost as volatiles during workup. Also, as a result of polymerization of degradation products, the long cooks— 12 h and greater—contained small amounts of black char that were removed during sample workup. The relative abundance of the monomer component remained low and declined steadily throughout the 40 h reaction period.

The degradation of **10** is accompanied by the formation of other DFDAs. The combined mass of other DFDAs in the reaction mixture at no time accounts fully for the loss of **10**; **10** does not degrade solely to DFDAs. Nevertheless, the mechanism of formation of DFDAs from inulin must incorporate "side reactions" to account for some isomerization of α-D-Fru*f*-1,2′:2,1′-β-D-Fru*f* to other DFDAs. By analogy we can expect other difuranose dianhydrides to behave similarly.

Also, it should be noted that the decline in the concentration of trimers (Figure 5), coincides with the initial increase and then decline in the concentration of DFDAs other than **10**. This implicates trimers as another possible source of the DFDAs that appeared.
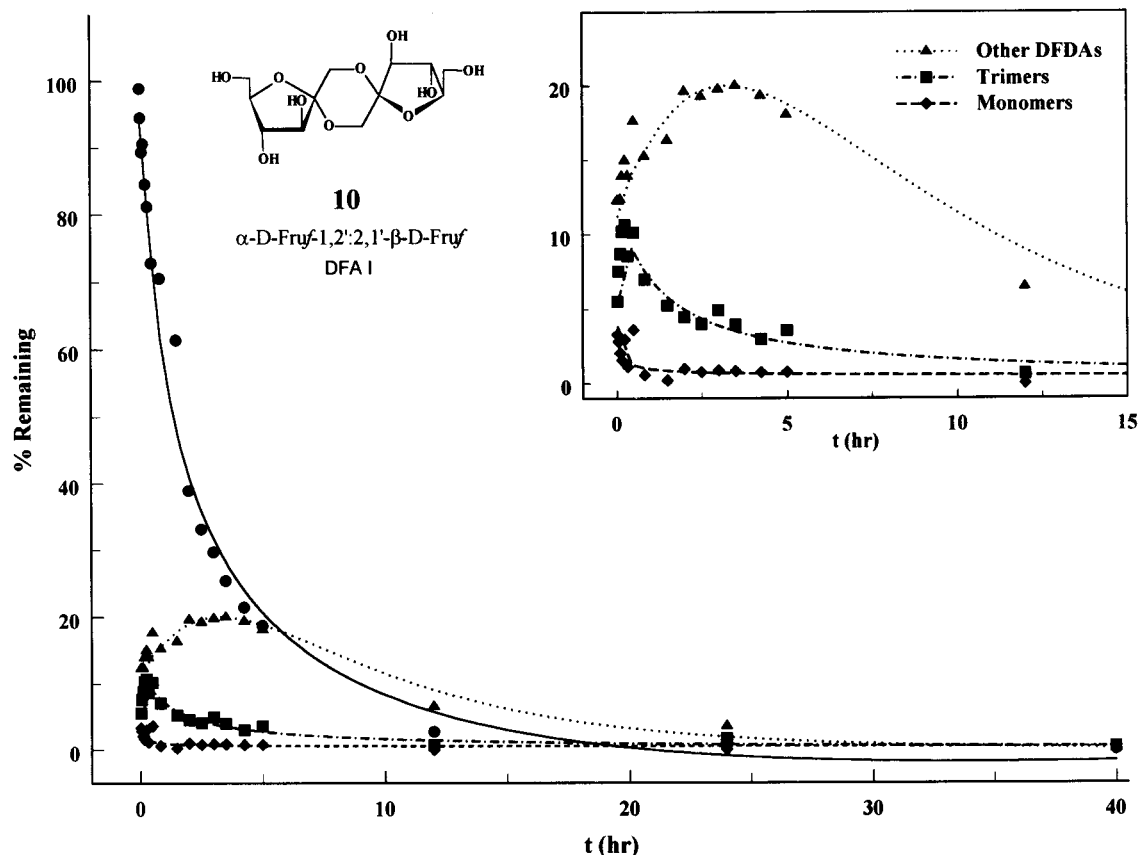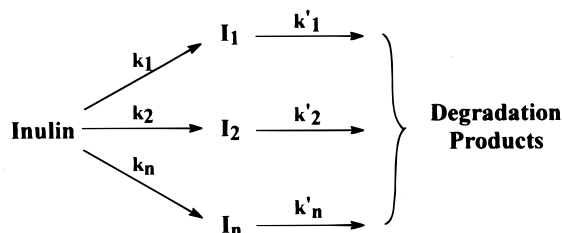
Figure 5. Thermolysis of α-D-Fru*f*-1,2′:2,1′-β-D-Fru*f* (**10**) at 160 °C in the presence of 1.5% citric acid.

Scheme 2. Model for Preliminary Curve Fitting

Kinetics of DFDA Formation and Decay. *Initial Rate Constant Estimates.* Initial estimates for growth and decay rate constants were obtained using nonlinear least-squares curve-fitting to weight percent conversion data for individual DFDAs. The rate equation for this treatment derives from a first-order parallel consecutive reaction mechanism shown in Scheme 2, where $I_{1,2\cdots n}$ represents DFDA$_{1,2\cdots n}$. Curve-fitting to the integrated rate eq 1 yielded "order of magnitude" estimates that provided starting points for numerical simulations. These estimates are most valid in the very early stages of thermolysis (0–20 min) while inulin still constitutes the primary source material. As mentioned, once inulin is depleted, DFDAs arise through isomerization and from sources other than inulin, for example, fructose.

After ∼30 min, the weight percent conversion data can be assumed to be dominated by the effects of degradation of DFDAs; the results observed with the degradation of **10** indicate that isomerization is a minor contributor. It was possible, therefore, to use the data to arrive at approximate rate constants for decay processes.

Nonlinear curve-fitting treatments of standard rate equations to data post 30 min suggested that DFDA decay occurs via both first- and second-order processes.

If degradation occurs via a first-order process, the rate law and its integrated solution are

$$-\frac{d[A]}{dt} = k[A] \Rightarrow [A]_t = [A]_0\,e^{-kt} \quad (2)$$

A nonlinear least-squares treatment of this equation for the inulin/1.5% citric acid/160 °C thermolysis data after 30 min for **10** overestimated the extent of degradation in the later stages but approximated the decay rate in the early stages fairly well.

Degradation may occur via a second-order process whereby a protonated dianhydride linkage opens to form a cationic species similar to **15**, which may then react

15
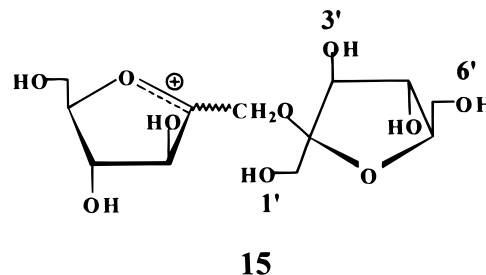
with OH-containing compounds. The general rate equation for this type of reaction is $v = k[A][B]$. This form of second-order kinetics is widely encountered, yet its application to the current study is far from straightforward. The nature of the analysis does not allow the identification of the second reactant, and a sensible graphical treatment is therefore not possible. Known possibilities for the second reactant include citric acid, which was added to the mixture, and inulin thermolysis products such as fructose, other DFDAs, glycosylated

Kinetics of Difructose Dianhydride Formation in Thermolysis of Inulin

J. Agric. Food Chem., Vol. 48, No. 5, 2000 **1831**

DFDAs, and nonspecific degradation products, for example, HMF.

Nonlinear curve-fitting to the rate equation $v = k[A]^2$ was carried out. The integrated form of this equation, after solving for $[A]_t$, is

$$[A]_t = [A]_0/(1 + [A]_0 kt) \qquad (3)$$

Nonlinear least-squares curve-fitting to eq 3 approximated the data after 20 h more closely than did eq 2, suggesting that second-order processes of some form may contribute. Equation 3 did not fit the earlier data as well as eq 2.

Effect of Temperature. Bond scission reactions of the type described in this work have high activation energies and are relatively more sensitive to temperature changes than other reaction types. Both the Arrhenius equation and transition state theory predict a strong temperature dependence for reactions with high activation energies. Also, since thermolysis occurred in viscous melts, there was some concern that diffusion control might be operating. A series of thermolysis experiments was conducted at elevated temperatures. At temperatures <160 °C the inulin/citric acid mixture does not liquefy smoothly and remains inhomogeneous for a significant time. Above 160 °C formation and decay of DFDAs from inulin are quite sensitive to temperature. As the temperature increases from 160 to 170 to 180 °C, the time at which maximum weight percent conversion occurs decreases from 25 to 15 to 5 min. The decay rate displays a similarly large temperature dependence.

Effect of Citric Acid Concentration on Weight Percent Conversion. In addition to the inulin/1.5% citric acid system, a number of experiments were conducted on mixtures of inulin with 1.0, 2.0, and 2.9% citric acid. Trends in the data for 1.0, 1.5, and 2.0% citric acid can be interpreted in terms of competing formation and decay rates for DFDAs, each dependent on $[H^+]$.
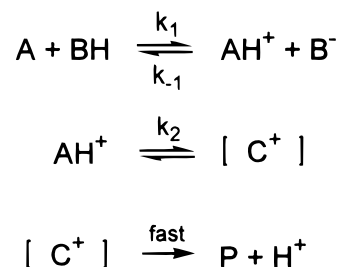
At a citric acid concentration of 1.0%, the DFDA decay rate is slow and the data described a smooth curve that gradually approached a maximum (at ~40−50 min). When citric acid was increased to 1.5%, the formation rate increased to an earlier maximum at 25−30 min. This earlier maximum indicates that the rate of decay is also increased. The slope of the curve after 30 min was negative, indicating that decay had become the dominant process. A higher maximum conversion for 1.5% citric acid was observed and may be due to a larger proportion of the starting material going toward DFDA formation, whereas in the 1.0% system less starting material goes into DFDA formation and more into reactions that result in non-DFDA products.

The formation rate at 2.0% citric acid was only slightly greater than that at 1.5%, which might indicate that a change to pseudo-order had occurred between 1.5 and 2.0%. A lower maximum conversion and slightly steeper decay indicated that degradation was competing more efficiently than in the 1.0 and 1.5% systems.

The observed trends for 1.0, 1.5, and 2.0% were maintained out to 5 h. The decay curves for these three descended toward equilibrium at relative rates in accord with citric acid concentration, that is, fastest descent for highest acid concentration.

The behavior of the 2.9% system was anomalous with a lower weight percent conversion than the other samples and an apparently reduced rate of degradation. This suggests a switch to different mechanisms; the low

Scheme 3. Model for Acid-Catalyzed Degradation of DFDAs

$$A + BH \underset{k_{-1}}{\overset{k_1}{\rightleftharpoons}} AH^+ + B^-$$

$$AH^+ \overset{k_2}{\rightleftharpoons} [\, C^+ \,]$$

$$[\, C^+ \,] \overset{fast}{\longrightarrow} P + H^+$$

weight percent conversion might be explained in terms of rapid removal of fructosyl moieties by acid-catalyzed dehydrations to give products that cannot give rise to DFDAs; this does not, however, explain the apparent decreased rate of degradation. This anomalous behavior was confirmed by inspection of the ratio of difuranose DFDAs to pyranose-containing DFDAs, which is higher and declines more slowly in the 2.9% system than in the other three systems. This seems to lend substance to the argument that different mechanisms are operating at the higher acid concentration.

pH during Thermolysis. There exists neither the instrumentation to measure nor the theory to explain the pH of high-temperature melts. Thus, a compromise was effected whereby an aqueous solution was prepared from a thermolysis product and the pH of that solution measured. These measurements can therefore only be regarded as indicators. A series of pH measurements was carried out in this fashion on thermolysis samples, including inulin/citric acid mixtures and pure citric acid, to establish whether a pseudo-first-order treatment was appropriate. Each sample (~10 mg) was subjected to the same thermolysis treatment as used throughout this study. The residues were dissolved in distilled H_2O (2.0 mL) and the pH recorded.

The color of the glassy citric acid residue changed during heating from light yellow after 30 min through yellow/orange to orange/brown after 9 h, indicating some degradation. However, the pH of pure citric acid was unaffected by heating at 160 °C for 9 h. The pH of the inulin/citric acid mixtures was also constant throughout the reaction time.

Role of Citric and Other Acids in DFDA Decay. Protonation and opening of an anhydride bond to form a carbocation (fructofuranose singly linked to a fructosyl cation) are analogous to the acid-catalyzed reactions of acetals and ketals (Espensen, 1995). A general scheme for acid-catalyzed degradation of DFDAs that incorporates these features is given in Scheme 3 in which A and AH^+ are the ketal and the protonated ketal (a difuranose DFDA in this case), respectively, BH is an organic acid, and B^- is the conjugate base. AH^+ opens to a carbocation C^+, which subsequently reacts rapidly to form products P.

If the first reaction in Scheme 3 is the rate-controlling step, the rate equation is (Espensen, 1995)

$$v = k_1[A][BH] \qquad (4)$$

The system will show *general* acid catalysis, and the rate will increase not with increasing hydrogen ion concentration but with the concentration of the acid. The concentrations of acidic byproducts of inulin thermolysis will also influence the rate.

1832 *J. Agric. Food Chem.,* Vol. 48, No. 5, 2000

Christian et al.

If the second reaction in Scheme 3 is the rate-controlling step, the rate equation is (Espensen, 1995)

$$v = (k_2/K_a^{AH})[A][H^+] \qquad (5)$$

The system will show *specific* acid catalysis, and the rate will depend on hydrogen ion concentration regardless of the source of the hydrogen ion. Aqueous acidified sucrose has been shown to undergo specific acid catalyzed hydrolysis. Mandal et al. (1986) found that the kinetic behavior of acid-catalyzed sucrose hydrolysis in four nonprotic solvents was similar to that in water and therefore assumed specific acid catalysis. Lönnberg and Gylén (1983) found the rate-limiting step in hydrolysis of alkyl fructofuranosides to be the formation of the fructosyl carbocation and not the protonation of the glycosidic oxygen. It is uncertain whether these results may be applied to anhydrous melts of inulin/citric acid. Experiments that monitor and control each acidic species present during thermolysis might resolve the question of whether DFDA formation and decay are catalyzed specifically by hydrogen ion. Lacking these experiments, we were forced to presume specific acid catalysis and develop the mechanistic model accordingly. In that case, protonation of the glycosidic oxygen (first step in Scheme 3) occurs rapidly, and formation of the carbocation is the rate-controlling step, assuming subsequent reaction of the carbocation is also fast. The overall kinetics will be pseudo-first-order because, as was demonstrated above, the pH remained constant throughout the course of the thermolysis. This does not rule out a contribution from other second-order mechanisms, for example, glycosylation to form trimers.

Conclusions upon Which Numerical Simulations Were Based. The data and information presented in the preceding sections lead to the following nine conclusions:

1. The fructosyl cation holds a central role in DFDA growth and decay. DFDAs, glycosylated DFDAs, and oligomers of inulin are ketals and will react via fructosyl cations under acidic conditions.

2. The major part of decay is pseudo-first-order; some second-order processes contribute to decay.

3. Five of the six difuranoses can form directly from inulin oligomers of dp > 2. Assuming protonation is rapid and there is no buildup of fructosyl cation, the formation of the cation will be the rate-controlling step and a simple, one-step mechanism (A → B) can be written for the formation of these five.

4. Four more DFDAs can form from inulin oligomers for which the fructofuranosyl cationic form has isomerized via the 2,6-anhydrofructose intermediate to the fructopyranosyl form.

5. The remaining five DFDAs do not contain β-D-fructofuranose rings and cannot form directly from inulin oligomers. In accordance with the ketal mechanism, isomerization provides a route to these five. The 2,6-anhydrofructose intermediate may play a role.

6. The pyranose-containing DFDAs do not appear to degrade significantly.

7. The difuranoses constitute >80% of the DFDAs at 30 min in the inulin/1.5% citric acid/160 °C system. Each is a possible "trickle" source for other DFDAs.

8. Isomerization might begin with a furanose/pyranose (instead of with a difuranose), in which case dipyranoses could form.

9. D-Fructose forms early and constitutes a source for DFDAs, especially those that cannot form from inulin.

Scheme 4. Formation of DFDA 10 Directly from Inulin

$$i \longrightarrow 10$$
$$i \longrightarrow sp$$
$$10 \longrightarrow sp$$
$$sp \longrightarrow 10$$
$$10 \longrightarrow np$$
$$10 + np \longrightarrow p$$
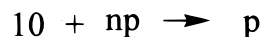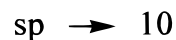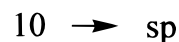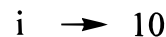
These conclusions were used to assemble the following four partial mechanisms. The division into four groups is based primarily on probable routes of formation. All data used in numerical simulations were taken from the inulin/1.5% citric acid/160 °C thermolysis samples.

DFDAs Directly from Inulin. Five of the six difuranoses (**1**, **3**, **5**, **10**, and **12**) can form directly from inulin. A mechanism for the formation and disappearance of **10** is shown is Scheme 4. This mechanism can equally apply to **1**, **3**, **5**, and **12**. DFDA **10** forms directly from inulin (i) and decays to nonspecific products (np). Inulin forms other DFDAs, designated specific products (sp), which represent a reservoir from which additional DFDAs may be added to the overall mechanism. Isomerization is represented by the two reactions **10** → sp and sp → **10**. The second-order decay pathway, **10** + np → p, arises from the following evidence. When thermolysis samples were dissolved in H_2O and chromatographed by SEC, one peak contained predominantly trimers. ES-MS of this fraction revealed a large peak corresponding to glycosylated DFDAs. Also, mild hydrolysis of this same trimer fraction in a previous inulin/citric acid thermolysis study (Manley-Harris and Richards, 1996) revealed a disproportionately greater abundance of difuranoses over pyranose-containing DFDAs. It is reasonable then to assume that some fraction of the disappearance of the difuranoses involves second-order reactions with fructosyl (or glucosyl) carbocations. For the purposes of this model the products (p) do not differ in nature from the nonspecific products (np). They are both nonspecific products but are labeled differently to avoid the implication that second-order decay is product-catalyzed. This model does not include a step whereby np or p can give rise to **10**.

Figure 6 compares numerical simulation of Scheme 4 to thermolysis data for DFDAs **1**, **3**, **5**, **10**, and **12**.

DFDAs from Inulin via the Anhydro Intermediate. The DFDAs that can form indirectly from inulin via the 2,6-anhydro intermediate are **2**, **4**, **7**, and **13**. The combined data for **6** and **7** are included in this group under the assumption that at any time during thermolysis **7** is the major contributor to weight percent conversion for the two. The justification for this lies in the fact that β-D-Frup-1,2′:2,1′-β-D-Frup, **14**, the only other dipyranose present, does not reach >~0.1% relative abundance at any time. At no point was Scheme 4 able to match the more gentle change from formation to decay near the maximum that **2**, **4**, **7**, and **13** exhibit without sacrificing the remainder of the fit. Inspection of the weight percent conversion plots for these DFDAs reveals a slower initial
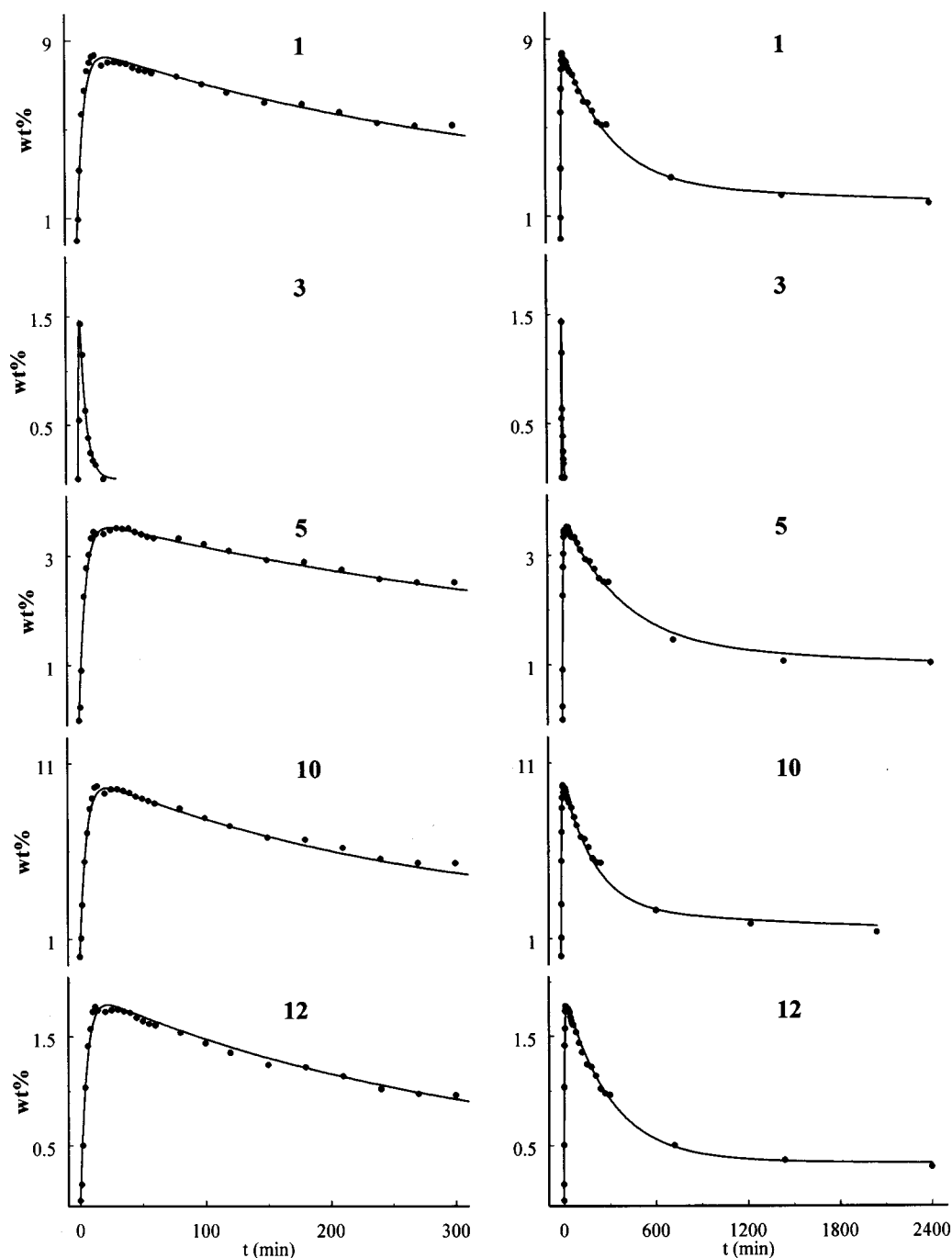
Kinetics of Difructose Dianhydride Formation in Thermolysis of Inulin

J. Agric. Food Chem., Vol. 48, No. 5, 2000 **1833**

Figure 6. Comparison between data and numerical simulation of Scheme 4 for difuranose DFDAs **1**, **3**, **5**, **10**, and **12**.

formation rate than for the difuranoses from the previous group (**1**, **3**, **5**, **10**, and **12**). The anhydro species could account for slower formation and is the obvious candidate for an additional rate-controlling step between inulin and this group. Including the anhydro species gives Scheme 5, which retains most of the features of the previous mechanism. The oligomeric 2,6-anhydro-D-fructose intermediate is designated an-i (anhydro-inulin). All other designations are the same. Many different values for the rate constant for second-order decay, DFDA + np → p, in this mechanism did not improve the fit over that obtained when this value was set to 0. This may be a reflection of the results obtained by Manley-Harris and Richards (1996) in which glycosylation of DFDAs favored the difuranoses over the pyranose-containing DFDAs. The primary OH

groups of a DFDA are less sterically hindered than the secondary OH groups and will react more easily with fructosyl carbocations. Incorporation of pyranose into DFDAs reduces the number of primary hydroxyls and thus the probability of glycosylation. Therefore, the second-order glycosylation process will be less important for **2**, **4**, **7**, and **13** and may be excluded from this mechanism with little adverse effect.

The simulated curves for Scheme 5 are presented in Figure 7. The early GC peak integration data for β-D-Fru$f$-2,1′:3,2′-α-D-Fru$p$, **2**, are unreliable due to low relative abundance and coelution with an unknown compound. There is a subtle indication of an induction period (lag time) in the data for these DFDAs; formation does not commence immediately from time zero. The introduction of the anhydro intermediate (an-i) into the
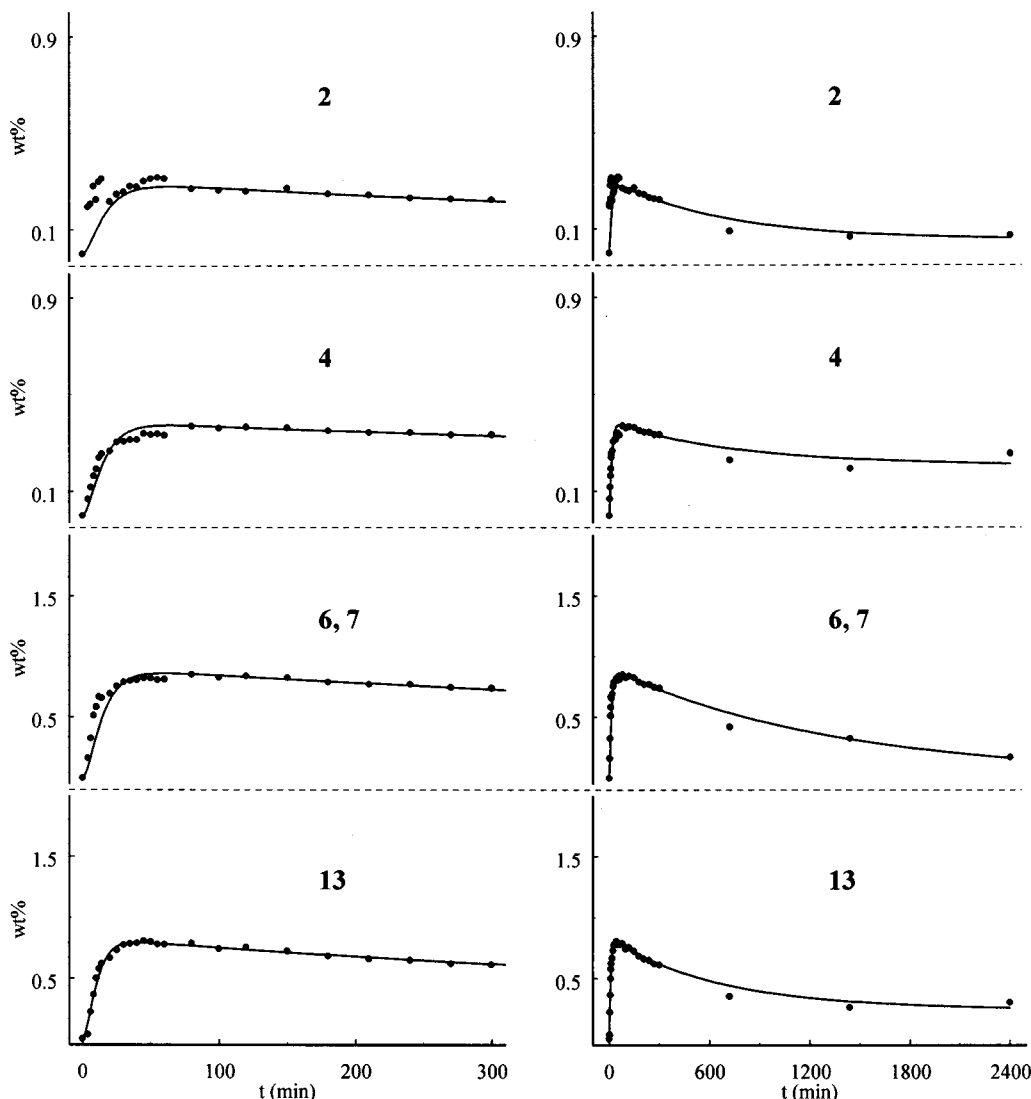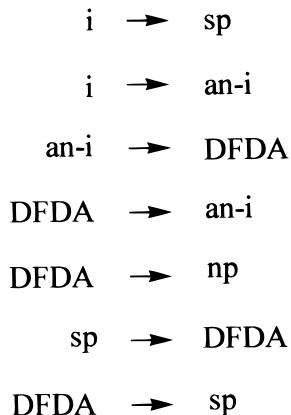
Figure 7. Comparison between data and numerical simulation of Scheme 5 for DFDAs **2**, **4**, **7**, and **13**.

Scheme 5. Formation of DFDAs 2, 4, 7, and 13 via the Anhydroinulin Species

i → sp

i → an-i

an-i → DFDA

DFDA → an-i

DFDA → np

sp → DFDA

DFDA → sp

mechanism provided some compensation for this feature. The curvature in and around maximum conversion also improved with the inclusion of the anhydro species. It was possible to match more closely the transition from growth to decay, which is less abrupt than in the difuranoses. However, Scheme 5 still cannot quite duplicate the formation rate in the early stages of the reaction.

The fit after ~1 h, when degradation has become the dominant process, out to ~5 h is very good; however, the 12 h data points all lie below the arc that describes a smooth continuation of the earlier data. Modifying rate constants to deepen the decay curvature to match the 12 h data sacrifices the earlier fit considerably. We assume that the 12 h data may be inaccurate.

Unique Mechanism for DFDA 8. DFDA **8** cannot form directly from inulin oligomers by intramolecular attack, because inulin contains only β anomers, and must arise rapidly from some other source that is present very early in the reaction. **10** forms early and could give rise to **8** via a one-step isomerization. Efforts to employ this isomerization in simulations failed to duplicate the rapid formation and decay rates that **8** exhibits.

HPAE-PED chromatograms of inulin indicate that some fructose is present very early in the thermolysis and that fructose concentration increases for the first 15 min of thermolysis. However, trial simulations using a second-order mechanism of the type 2 fructose → DFDA also failed to match the data. This type of mechanism, in combination with the same decay pathways used in previous mechanisms, yields a conversion plot with a more gentle transition from growth to decay. The initial formation rate is too slow, and the change
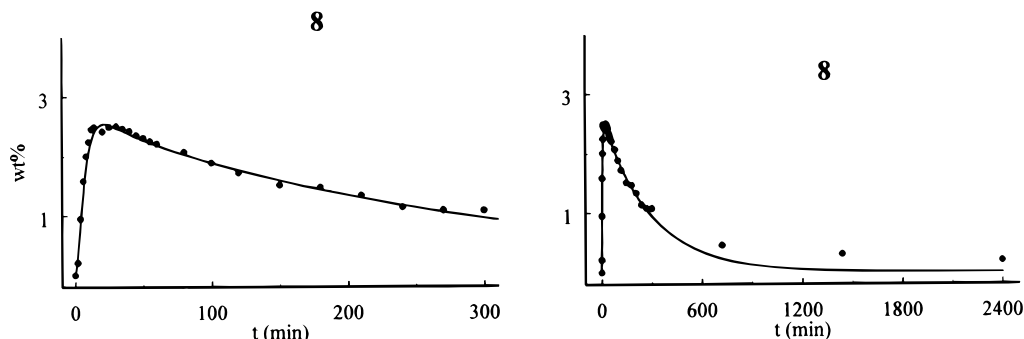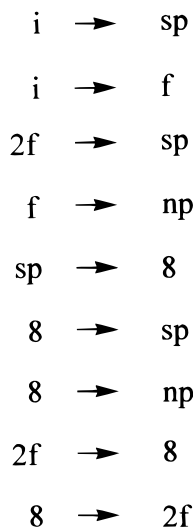
Kinetics of Difructose Dianhydride Formation in Thermolysis of Inulin

J. Agric. Food Chem., Vol. 48, No. 5, 2000 **1835**

Figure 8. Comparison between data and numerical simulation of Scheme 6 for difuranose DFDA **8**.

Scheme 6. DFDA 8 from Isomerization and from Bimolecular Reaction of Fructose

$$i \longrightarrow sp$$
$$i \longrightarrow f$$
$$2f \longrightarrow sp$$
$$f \longrightarrow np$$
$$sp \longrightarrow 8$$
$$8 \longrightarrow sp$$
$$8 \longrightarrow np$$
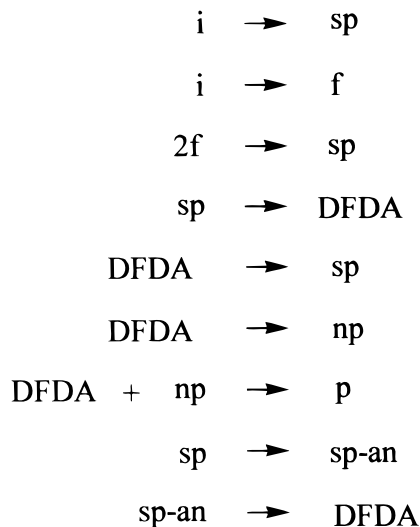$$2f \longrightarrow 8$$
$$8 \longrightarrow 2f$$

from positive to negative slope at the maximum is not abrupt enough.

Formation by both first-order isomerization and second-order bimolecular reaction of fructose are incorporated into Scheme 6. A portion of inulin in this mechanism goes toward production of fructose, which may go on to form **8** and other DFDAs (sp) or degrade to nonspecific products (np). The large first-order decay rate constants that were necessary to duplicate the steep decline from maximum conversion completely overshadowed the minimal contribution from the second-order pathway $8 + np \rightarrow p$. This path was therefore excluded from the mechanism.

The simulation of weight percent conversion data for DFDA **8** according to Scheme 6 is presented in Figure 8. The curve matches the data well for the first 5 h. There is an almost imperceptible induction period followed by rapid growth and decay. The simulation out to 5 h is as good as or better than those for the other difuranoses. However, as mentioned, large decay constants were necessary to obtain this early fit. This resulted in almost complete disappearance of this DFDA after ~25 h, even though the data specify a more gradual decay to a small but definite concentration at 40 h.

Additional Anhydro Species. DFDAs other than the one in question (sp) may form anhydro species (sp-an) via the carbocation. These anhydro species may then go on to form the DFDA under scrutiny (Scheme 7). This is analogous to the previously mentioned mechanism whereby inulin forms the anhydro species (an-i). This

Scheme 7. Formation of DFDAs 9, 11, and 14

$$i \longrightarrow sp$$
$$i \longrightarrow f$$
$$2f \longrightarrow sp$$
$$sp \longrightarrow DFDA$$
$$DFDA \longrightarrow sp$$
$$DFDA \longrightarrow np$$
$$DFDA + np \longrightarrow p$$
$$sp \longrightarrow sp\text{-}an$$
$$sp\text{-}an \longrightarrow DFDA$$

mechanism was applied to **9**, **11**, and **14** with more success than previous attempts to model these DFDAs but with less overall success than for those DFDAs that form from inulin.

The simulated curves for **9**, **11**, and **14** are presented in Figure 9. The initial formation rate for **9** is too rapid to be modeled accurately by this mechanism. Increasing the first-order formation rate to match the data in the 0–20 min region causes the simulated curve to rise well above the actual maximum. It was not possible to correct for this by increasing decay rates without completely sacrificing the fit in the 1–5 h range and overestimating the extent of decay. The earlier observations concerning the validity of the 12 h data were reinforced by the results of modeling of these compounds.

Analysis of Commercial Chicory Samples. Four samples were used: high-roast (HR) and medium-roast (MR) chicory and instant HR and MR chicory derived by hot-water extraction and spray-drying. The definitions of high and medium roast relate to the duration of roasting, ~20 and ~10 min, respectively, rather than to temperature (140–145 °C for both). The instant samples and the methanol extract of the HR and MR chicories were all fractionated by SEC using LC method iv. The fractions were then analyzed by ES-MS. In addition, the instant samples were silylated and analyzed by GC-FID and GC-MS.

The ES-MS of all samples revealed two series of ions, those corresponding to singly linked oligosaccharides and those corresponding to oligomers formed by addition of glycosyl units to di-D-fructose dianhydrides. The effect of a dianhydride moiety in an oligomer is to lower
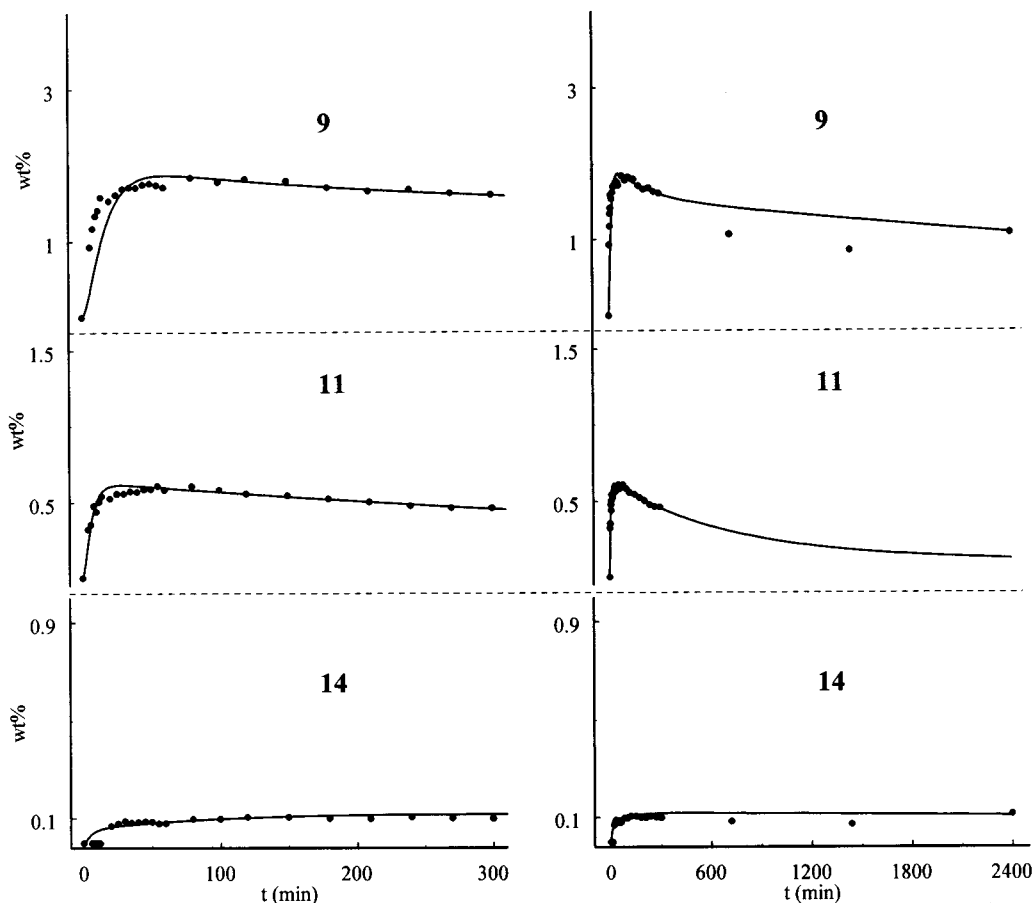
Figure 9. Comparison between data and numerical simulation of Scheme 7 for DFDAs **9**, **11**, and **14**.

the molecular mass by 18 Da. In the medium roast, shorter duration sample the ions corresponding to singly linked oligosaccharides predominated and structures of up to dp 12 were observed. In contrast, the HR sample showed structures of only up to dp 8 and ions corresponding to dianhydride-containing oligomers predominated. GC-FID and GC-MS of the instant MR sample showed that the major peak in the dimer fraction was sucrose, although α-D-Fru*f*-1,2′:2,3′-β-D-Fru*f*, **1**, β-D-Fru*f*-1,2′:2,3′-β-D-Fru*f*, **5**, α-D-Fru*f*-1,2′:2,1′-β-D-Fru*f*, **10**, and β-D-Fru*f*-1,2′:2,1′-β-D-Fru*f*, **12**, were also observed. In the instant HR sample the major peaks in the dimer fraction were α-D-Fru*f*-1,2′:2,3′-β-D-Fru*f*, **1**, and α-D-Fru*f*-1,2′:2,1′-β-D-Fru*f*, **10**. β-D-Fru*f*-1,2′:2,3′-β-D-Fru*f*, **5**, α-D-Fru*f*-1,2′:2,1′-α-D-Fru*f*, **8**, and β-D-Fru*f*-1,2′:2,1′-β-D-Fru*f*, **12**, were also observed. These are the DFDAs that are predicted to form early by the model inulin/citric acid system, which also predicts that **1** and **10** will be the major DFDA products.

SEC fractionation and ES-MS of the methanol extract of MR chicory gave results similar to those obtained from the instant MR sample except for a reduction in higher oligosaccharide material. However, similar treatment of the methanol extract of the HR chicory revealed a new series of ions corresponding to multiply dehydrated oligomers, ions such as Da/e 275, 311, and 383; ions at Da/e 119 and 149 corresponding to furaldehyde and 5-hydroxymethylfurfural (5-HMF), respectively, were also observed. Multiply dehydrated structures may arise from successive dehydration of oligomers or by oligomerization of degradation products such as 5-HMF on the way to formation of humins; they would be expected to be more soluble in methanol than in water

and thus not be present to the same extent in the instant sample, which is an aqueous extract.

The main storage polysaccharide of chicory is inulin, and up to 3% of organic acids have also been identified in chicory roots (Pazola, 1985); therefore, the conditions chosen for roasting chicory are such as almost to optimize the formation of di-D-fructose dianhydrides. The presence of sucrose in the shorter duration roasts and its disappearance thereafter correspond to observations made in the model thermolyses in this study, as does the decrease in the singly linked oligosaccharides, presumably inulin, as the duration of heating increases. The multiply dehydrated ion series have not been observed in ES-MS of model thermolyses. Chicory is a much more complex system, and possibly other components, lacking in the simple model systems, catalyze such dehydrations.

Conclusions. The thermolysis of inulin in the presence of citric acid leads to a complex series of reactions giving rise to 14 di-D-fructose dianhydrides and oligomers arising by addition of glycosyl residues to these. With one exception the earliest formed DFDAs can be shown, by modeling, to form directly from inulin. However, inulin is completely consumed early in the reaction, and other sources are required to account for the continuing formation of these DFDAs and to account for those DFDA species that cannot form directly from inulin. Other possible sources include fructose, sucrose, and isomerization of difuranose DFDAs. The simple inulin/citric acid system serves as a model for the commercial roasting of chicory but cannot account for the multiple dehydrations observed when more prolonged roasting is employed.

Supporting Information Available: Figures 1−8 and Table 1 illustrate the effects of thermolysis at 160 °C upon inulin and upon DFDAs **6** and **9**, the effects upon thermolysis of changing citric acid concentration and temperature and the attempted fit of a nonlinear least-squares curve to data for the decay of DFDA **10**. Also available are electrospray-mass spectra of selected fractions variously processed chicory. This material is available free of charge via the Internet at http://pubs.acs.org.

LITERATURE CITED

Angyal, S. J.; Bethell, G. S. Conformational analysis in carbohydrate chemistry. III. The ^{13}C NMR spectra of the hexuloses. *Aust. J. Chem.* **1976**, *29*, 1249−1265.

Angyal, S. J.; Craig, D. C.; Defaye, J.; Gadelle, A. Complexes of carbohydrates with metal cations. XVI. Di-D-fructose dianhydrides and di-L-sorbose dianhydrides. *Can. J. Chem.* **1990**, *68*, 1140−1144.

Blakeney, A. B.; Harris, P. J.; Henry, R. J.; Stone, B. A. A simple and rapid preparation of alditol acetates for monosaccharide analysis. *Carbohydr. Res.* **1983**, *113*, 291−299.

Blize, A. E.; Manley-Harris, M.; Richards, G. N. Di-D-fructose dianhydrides from the pyrolysis of inulin. *Carbohydr. Res.* **1994**, *265*, 31−39.

Bock, K.; Pedersen, C.; Pedersen, H. Carbon-13 nuclear magnetic resonance data for oligosaccharides. *Adv. Carbohydr. Chem. Biochem.* **1984**, *42*, 193−225.

Carpita, N. C.; Shea, E. M. Linkage structures of carbohydrates by gas chromatography−mass spectrometry (GC-MS) of partially methylated alditol acetates. In *Analysis of Carbohydrates by GLC and MS*; Biermann, C. J., McGinnis, G. D., Eds.; CRC Press: Boca Raton, FL, 1988.

Ciucanu, I. O.; Kerek, F. A simple and rapid method for the permethylation of carbohydrates. *Carbohydr. Res.* **1984**, *131*, 209−217.

Cuthbert, D.; Wood, F. S.; Gorman, J. W. *Fitting Equations to Data. Computer Analysis of Multifactor Data for Scientists and Engineers*; Wiley-Interscience: New York, 1971.

Defaye, J.; Fernández, J. M. G. Selective protonic activation of isomeric glycosylfructoses with pyridinium poly(hydrogen fluoride) and synthesis of spirodioxanyl oligosaccharides. *Carbohydr. Res.* **1992**, *237*, 223−247.

Defaye, J.; Fernández, J. M. G. The oligosaccharide components of caramel. *Zuckerindustrie* **1995**, *120*, 700−704.

Dionex Corp., 1228 Titan Way, P.O. Box 3603, Sunnyvale, CA 94088-3603.

Espensen, J. H. *Chemical Kinetics and Reaction Mechanisms*, 2nd ed.; McGraw-Hill: New York, 1995.

Gibson, G. R.; Roberfroid, M. B. Dietary modulation of the human colonic microbiota: Introducing the concept of prebiotics. *J. Nutr.* **1995**, *125*, 1401−1412.

Goretti, G.; Liberti, A.; Di Pablo, C. Gas chromatographic investigation on caramel aroma. *Ann. Chim.* **1980**, *70*, 277−284.

Hilton, H. W. Di-D-fructose Dianhydrides. In *Methods in Carbohydrate Chemistry*; Whistler, R. L., Wolfrom, M. L., BeMiller, J. N., Eds.; Academic Press: New York, 1963; pp 199−203.

Lönnberg, H.; Gylén, O. The acid-catalyzed hydrolysis of anomeric alkyl fructofuranosides. *J. Carbohydr. Chem.* **1983**, *2*, 177−188.

Mandal, U.; Das, K.; Kundu, K. K. Kinetic solvent effects on acid-catalyzed hydrolysis of sucrose in aqueous mixtures of some protic, aprotic, and dipolar aprotic solvents. *Can. J. Chem.* **1986**, *64*, 1638−1642.

Manley-Harris, M.; Richards, G. N. A novel fructoglucan from the thermal polymerization of sucrose. *Carbohydr. Res.* **1993**, *240*, 183−196.

Manley-Harris, M.; Richards, G. N. Di-D-fructose dianhydrides and related oligomers from thermal treatments of inulin and sucrose. *Carbohydr. Res.* **1996**, *287*, 183−202.

Manley-Harris, M.; Richards, G. N. Dihexulose Dianhydrides. *Adv. Carbohydr. Chem. Biochem.* **1997**, *52*, 207−266.

Matsuyama, T.; Tanaka, K.; Uchiyama, T. Isolation and identification of the *Aspergillus fumigatus* difructose dianhydride. *Agric. Biol. Chem.* **1991**, *55*, 1413−1414.

Needs, P. W.; Selvendran, R. R. Avoiding oxidative degradation during sodium hydroxide/methyl iodide-mediated carbohydrate methylation in dimethyl sulfoxide. *Carbohydr. Res.* **1993**, *245*, 1−10.

Orban, J. I.; Patterson, J. A.; Sutton, A. L.; Richards, G. N. Effect of sucrose thermal oligosaccharide caramel, dietary vitamin-mineral level, and brooding temperature on growth and intestinal bacterial populations of broiler chickens. *Poult. Sci.* **1997**, *76*, 482−490.

Pazola, Z. In *Coffee. Vol. 5: Related Beverages*; Clarke, R. J., Macrae, R., Eds.; Elsevier: London, U.K., 1985; pp 19−57.

Ponder, G. R.; Richards, G. N. Pyrolysis of inulin, glucose, and fructose. *Carbohydr. Res.* **1993**, *244*, 341−359.

Ratsimba, V.; Fernández, J. M. G.; Defaye, J.; Nigay, H.; Voilley, A. Qualitative and quantitative evaluation of mono- and disaccharides in D-fructose, D-glucose and sucrose caramels by gas−liquid chromatography−mass spectrometry. Di-D-fructose dianhydrides as tracers of caramel authenticity. *J. Chromatogr. A* **1999**, *844*, 283−293.

Scheer, M. D. Thermal dehydration kinetics of disaccharides. *Int. J. Chem. Kinet.* **1983**, *15*, 141−149.

Slaughter, L. H.; Livingston, D. P. Separation of fructan isomers by high performance anion exchange chromatography. *Carbohydr. Res.* **1994**, *253*, 287−291.